

Invited paper

UVB/UVC induced processes in model DNA helices studied by time-resolved spectroscopy: Pitfalls and tricks

Dimitra Markovitsi*, Delphine Onidas, Francis Talbot, Sylvie Marguet,
Thomas Gustavsson, Elodie Lazzarotto

Laboratoire Francis Perrin, CEA/DSM/DRECAM/SPAM-CNRS URA 2453, CEA Saclay, F-91191 Gif-sur-Yvette, France

Received 26 April 2006; received in revised form 23 May 2006; accepted 29 May 2006

Available online 7 July 2006

Abstract

The investigation of model DNA helices using time-resolved absorption and fluorescence spectroscopy with UVB/UVC excitation knows currently an increasing interest due, in particular, to the use of femtosecond spectroscopy. The study of such complex and fragile systems presents specific difficulties which are not encountered in the experiments performed on the monomeric DNA units. They are related both to the quality of the DNA helices and their sensitivity towards UV radiation. The present paper tackles some of these problems (pitfalls) and describes experimental protocols developed in our laboratory in order to overcome them (tricks). We focus on experiments carried out by fluorescence upconversion spectroscopy, time-correlated single photon counting and nanosecond flash photolysis. We illustrate our experience with examples obtained for double helices containing only adenine–thymine base pairs. We consider this report of pitfalls and tricks, which is far from being complete, as a first step towards a codification of rules for time-resolved studies with model DNA helices. This codification has to be established by common agreement of the various groups working in the field.

© 2006 Elsevier B.V. All rights reserved.

Keywords: DNA photodamage; DNA fluorescence; DNA transient absorption; DNA excitons; DNA excited states; DNA energy transfer; Time-resolved spectroscopy; Experimental artifacts

1. Introduction

UV irradiation absorbed by the DNA bases induces photochemical reactions leading to carcinogenic mutations [1,2]. Numerous studies describe the major photoproducts such as bipyrimidine dimers (cyclobutanes and (6–4) photoadducts), 6-hydroxy-5,6-dihydrocytosine or 8-oxo-7-8-dihydroguanine [3,4]. However, the time-scales at which these photoreactions occur, as well as the nature of the excited states intervening between photon absorption and the formation of a given photoproduct remain poorly understood. It is worth-noticing that the first time-resolved investigation dealing with the formation of photoproducts was reported only last year [5]. The main finding of that work is that the (6–4) thymine photo-adducts are formed within 4 ms via a reaction intermediate. Although experiments on this time-scale were technically feasible already 40 years

ago [6], specific difficulties related to the complexity and the fragility of DNA helices towards UV radiation prevented them from being studied.

Spectroscopic studies aiming at the understanding of fundamental processes in complex systems are highly facilitated if the various components of the system can be excited selectively. This is not the case for DNA double helices because the lowest energy absorption band of adenine, thymine, cytosine and guanine and of the corresponding nucleosides and nucleotides are all located around 260 nm and overlap strongly [7,8]. Moreover, many of the photoproducts absorb also in the same spectral region and, therefore, it is nearly impossible to clearly identify them in a transient absorption spectrum. The “puzzle” may become somewhat easier if, instead of natural DNA, single stranded or double stranded synthetic model helices, with simple base sequence, such as $(dA)_n$, $(dT)_n$, $(dC)_n$, $(dA)_n \cdot (dT)_n$, $(dAdT)_n \cdot (dAdT)_n$ or $(dCdG)_n \cdot (dCdG)_n$, are considered.

Regarding the singlet excited states and the associated energy transfer processes, investigations have for long suffered from the limited time resolution. The lifetimes of the lowest singlet

* Corresponding author. Tel.: +33 1 69 08 46 44; fax: +33 1 69 08 46 44.
E-mail address: dimitra.markovitsi@cea.fr (D. Markovitsi).

excited states of the monomeric DNA units (bases, nucleosides and nucleotides) were determined a few years ago using femtosecond transient absorption and fluorescence upconversion techniques [8–15]. In 2003 appeared the first time-resolved fluorescence study of DNA oligomers with femtosecond resolution; it showed that organization of nucleotides in single and double helices, (dA)₂₀, (dT)₂₀ and (dA)₂₀·(dT)₂₀, renders the fluorescence decays progressively slower [16]. More recently, the fluorescence of similar double helices, poly(dA)·poly(dT), induced by femtosecond pulses, was probed by fluorescence upconversion and time-correlated single photon counting (TCSPC) over a large time domain (100 fs to 100 ns) [17]. The time behaviour of the fluorescence, associated with the steady-state absorption and fluorescence spectra, was explained by the formation of Franck–Condon states delocalized over several bases and the subsequent energy transfer occurring faster than 100 fs [17]. In parallel, a transient absorption study with femtosecond resolution reported the existence of important slow components (50–150 ps) in the decays of (dA)₁₈, (dA)₁₈·(dT)₁₈ and (dAdT)₉·(dAdT)₉. The authors assign the slow components to adenine excimers and draw the conclusion that these limit excitation energy to one strand at a time [18]. This interpretation as well as the comparison between transient absorption and fluorescence data are currently under discussion [19].

The accumulation of fluorescence data concerning the double helices (dA)_n·(dT)_n has contributed to increase the confusion about the properties of their excited states. These fluorescence studies were performed for helices with various numbers of base pairs ($n = 15$ [20], $n = 20$ [16,19,21] and $n > 1000$ [17,21]) using different experimental setups (TCSPC with excitation at 293 nm [21], streak camera with excitation at 283 nm [20], upconversion and TCSPC with excitation at 267 nm [16,17,19]). Thus, one can wonder whether the helix length or the excitation wavelength plays a crucial role on the nature of the emitting states.

Our recent work on model DNA helices by three different time-resolved techniques, fluorescence upconversion, TCSPC and nanosecond flash photolysis [5,16,17,19,22,23] has made us aware of certain “pitfalls” which may lead to a complete misinterpretation of the experimental results. These pitfalls mainly concern the quality of the DNA helices and re-excitation of helices containing photoproducts.

In the case of DNA helices with simple repetitive sequences, base pairing is often incomplete. As a consequence, solutions of these compounds may contain not only double strands, but also a certain amount of unpaired bases. Furthermore, the above-mentioned systems are commercially available with a certain degree of purity. This is largely appropriate for most applications, but insufficient when their fluorescence properties are studied. This is understandable taking into account that the fluorescence quantum yield of nucleic acids is only of the order of 10^{-4} [4]. Infinitesimal traces of highly fluorescent impurities may give rise to fluorescence signals comparable to or stronger than those of the DNA helices.

The transient absorption and fluorescence signals of DNA model helices are usually very weak and necessitate averaging over a large number of laser shots. It is possible that repetitive laser pulses excite DNA helices which have already under-

gone a photochemical reaction. The presence of a lesion may change the transient signals in two ways. The formation of a photoproduct, such as a thymine dimer, within a double helix disrupts base pairing and base stacking and induces conformational changes around the lesion. The electronic coupling which governs the properties of the excited states delocalized over several bases [17,24–28] is thus altered. As a consequence, the whole cascade of processes, including excited state relaxation, is expected to change as well. In addition, the proper signals (transient absorption or fluorescence) of a photoproduct may be superposed to those of the unaltered helices. The situation is further complicated by the fact that laser excitation of a model helix gives rise to variety of photoproducts whose relative ratios depend on the pulse intensity. Indeed, radical cations of the bases, formed following ionization the DNA helix, lead to different types of photoproducts than those resulting from electronic excited states. We have shown quite recently that the quantum yield for one photon ionization of double helices containing only adenine–thymine pairs at 266 nm is of the order of 10^{-3} [23]. Upon increasing the laser intensity, two photon ionization prevails and, consequently, the ratio of the various photoproducts changes [29]. The photophysical and photochemical properties of all these photoproducts are, in general, not well characterized.

In order to overcome the problems described above, we have developed specific experimental protocols (tricks). Usually the pitfalls are not explicitly mentioned in the articles and the tricks are hidden among various experimental details. Trying to compare our data with those obtained by other groups, we have not been able to figure out whether these problems had been resolved or not. The purpose of the present paper is to explicitly point out some of the pitfalls encountered in our studies, describe their effect on the measured signals and show how the adopted tricks contribute to improve the quality of the data.

2. Apparatus and experimental setups

Steady-state absorption and fluorescence spectra were recorded with a Perkin Lambda 900 and a SPEX Fluorolog-2 spectrofluorometer, respectively, according to the procedure reported in reference [8].

The time-resolved fluorescence measurements used as excitation source the third harmonic of a mode-locked Ti-sapphire laser (Coherent MIRA 900; 267 nm). The repetition rate was 76 MHz for upconversion measurements but, for time-correlated single photon counting operation, it was reduced to 236 kHz by means of a pulse-picker (Coherent Model 9200).

The fluorescence upconversion setup is described in detail elsewhere [12,13]. Temporal scans were made in both parallel (I_{par}) and perpendicular (I_{perp}) mode by controlling the polarization of the exciting beam with a half-wave plate. The instrumental response function was about 400 fs (fwhm).

The time-correlated single photon counting setup used a Becker & Hickl GmbH SPC630 card. Fluorescence was detected by a microchannel plate (R1564 U Hamamatsu) placed after a SPEX monochromator. Scattered excitation light was blocked by a Schott WG 295 filter. The instrumental response function

was 60 ps (fwhm). Parallel and perpendicular components were determined by means of a Glan Thomson prism.

For both upconversion and TCSPC, the total fluorescence decays $F(t)$ were calculated according to: $F(t) = I_{\text{par}}(t) + 2GI_{\text{perp}}(t)$, where G accounts for the polarisation dependent sensitivity of the detection system.

Laser flash photolysis experiments were performed using the fourth harmonic (266 nm, 8 ns) of a Nd:YAG laser (Spectra-Physics Quanta Ray). The repetition rate was 2 Hz. The probing light (450 W Xenon arc) was observed at right angle with respect to the exciting beam, dispersed in a SPEX monochromator, detected by a Hamamatsu R938T photomultiplier and analyzed by a Tektronix DSA 620 oscilloscope.

The power of the femtosecond laser was measured by a powermeter (Melles Griot 13PEM001), whereas the energy of the nanosecond laser pulses was determined by an energy radiometer (Laser precision Instruments, Rj 7200).

All the time-resolved data presented were obtained at 20 °C.

3. Quality of DNA helices

In this section we describe two problems we encountered regarding the quality of the DNA helices. First, we examine how absorption spectroscopy can shed some light on the efficiency of base pairing. We discuss our observations in the light of theoretical calculations dealing with the nature of the excited states of these systems. The second problem concerns the presence of fluorescent impurities, whose identification is not obvious and necessitates thorough steady-state fluorescence studies.

3.1. Base pairing

The double stranded polymers, poly(dA)·poly(dT) (ca. 2000 bp) and poly(dAdT)·poly(dAdT) (200–400 bp), were purchased from Amersham Biosciences and were delivered as lyophilised pellets. These pellets were dissolved in phosphate buffer in order to obtain a concentration of ca. 0.005 M per base. Complete dissolution was achieved by immersing a small Pyrex flask containing the solution into the water bath (3 l) of a temperature controller LAUD A ECOLINE 003, heated at 90 °C. After 5 min, the heating was stopped and the bath was cooled slowly to 20 °C while circulating the water of the heat bath. The annealing was systematically repeated for solutions stored at –20 °C prior to any spectroscopic measurement. When these protocols were followed, the absorption spectra of each double helix, recorded with 0.2 nm steps, were reproducible.

The double stranded oligomers (dA)₂₀·(dT)₂₀, (dAdT)₁₀·(dAdT)₁₀ and (dA)₉(dT)₂(dA)₉·(dT)₉(dA)₂(dT)₉ were purchased from Eurogentec. After annealing, they had been purified by polyacrylamide gel electrophoresis (PAGE) and delivered to us in phosphate buffer at a concentration of about 0.1 M per base. We simply diluted them in order to obtain concentrations appropriate to each type of experiment. Submitting the oligomer solutions to the heat treatment described above did not induce any noticeable change in their absorption spectra.

The experimental curves presented here for both polymers and oligomers were obtained for concentrations ranging from

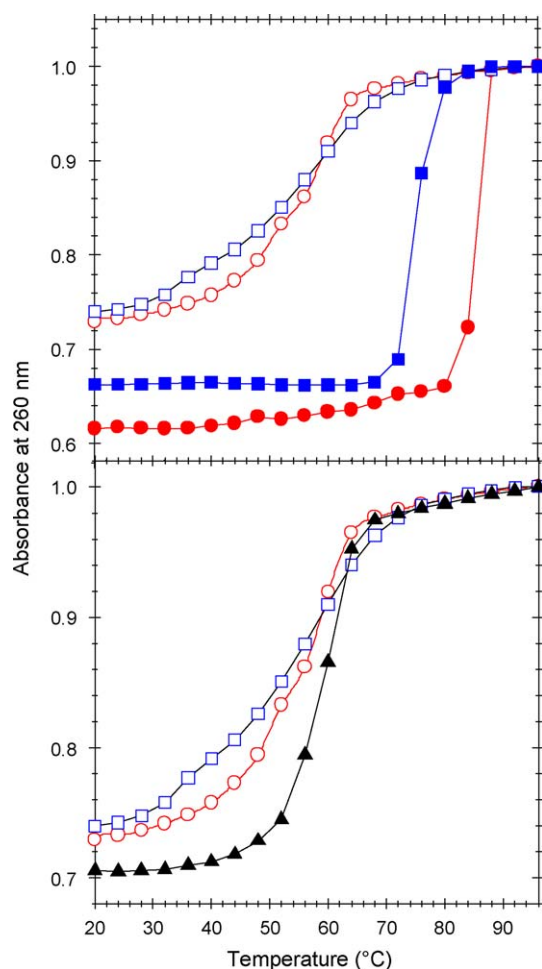


Fig. 1. Melting curves obtained for oligomeric and polymeric double helices: (dA)₂₀·(dT)₂₀ (open circles), poly(dA)·poly(dT) (full circles), (dAdT)₁₀·(dAdT)₁₀ (open squares), poly(dAdT)·poly(dAdT) (full squares), (dA)₉(dT)₂(dA)₉·(dT)₉(dA)₂(dT)₉ (triangles).

10^{-5} to 2×10^{-3} M (per base) using the same type of buffer (pH 6.8; 0.1 M NaH₂PO₄, 0.1 M Na₂HPO₄, 0.25 M NaCl). Under these conditions, the ionic strength, which greatly affects the conformation of double helices, was controlled by the buffer.

We recorded the absorption spectra as a function of temperature. The melting curves, determined from the absorbance at 260 nm, are shown in Fig. 1. As expected, the melting temperature increases with the number of base pairs (upper panel in Fig. 1): it is around 55 °C for (dA)₂₀·(dT)₂₀ and (dAdT)₁₀·(dAdT)₁₀ with 20 bp, 75 °C for poly(dAdT)·poly(dAdT) (200–400 bp) and 86 °C for poly(dA)·poly(dT) (2000 bp). The melting of the oligomers is less sharp than that of the polymers and indicates a greater polydispersity regarding the number of base pairs. This polydispersity arises mainly from a slipping of one strand with respect to the other. As a matter of fact, the melting curve of (dA)₉(dT)₂(dA)₉·(dT)₉(dA)₂(dT)₉; composed, like (dA)₂₀·(dT)₂₀, of 20 adenine–thymine base pairs is sharper than those of the oligomers with strictly repetitive sequence (lower panel in Fig. 1). Clearly, the presence of an inversion in the base sequence locks the relative position of the two strands.

Table 1
Absorption maxima and hypochromism of double helices

Compound	λ_{\max} (nm) ^a	H_{260} (%) ^b
(dA) ₂₀ ·(dT) ₂₀	259.4	27.0
(dAdT) ₁₀ ·(dAdT) ₁₀	262.4	26.0
(dA) ₉ (dT) ₂ (dA) ₉ ·(dT) ₉ (dA) ₂ (dT) ₉	259.0	29.4
Poly(dA)·poly(dT)	258.8	38.4
Poly(dAdT)·poly(dAdT)	262.6	33.7

^a Precision: 0.2 nm.

^b $H_{260} = (A_{96^\circ\text{C}} - A_{20^\circ\text{C}})/A_{96^\circ\text{C}}$; $A_{20^\circ\text{C}}$ and $A_{96^\circ\text{C}}$ denote the absorbance at 260 nm recorded at 20 and 96 °C, respectively.

The difference between the absorbance recorded at the highest and lowest temperature is more important for the polymers compared to the oligomers with the same sequence (upper panel in Fig. 1). We have quantified the hypochromism of our double helices by calculating the quantity $H_{260} = (A_{96^\circ\text{C}} - A_{20^\circ\text{C}})/A_{96^\circ\text{C}}$, where $A_{20^\circ\text{C}}$ and $A_{96^\circ\text{C}}$ denote the absorbance at 20 and 96 °C, respectively, measured at 260 nm (Table 1). The H_{260} value found for poly(dA)·poly(dT) is higher than that found for poly(dAdT)·poly(dAdT), in agreement with the molar extinction coefficients reported in the literature for these two polymers [30,31]. For both sequences, the oligomers exhibit a lower hypochromism than the polymers. The hypochromism of (dA)₉(dT)₂(dA)₉·(dT)₉(dA)₂(dT)₉ (29.4%) is higher than that of (dA)₂₀·(dT)₂₀ (27%).

It is interesting to correlate the characteristics of the melting curves with the absorption spectra and the nature of the excited states of the examined helices. The normalized absorption spectra of the two oligomers and the two polymers are shown in Fig. 2. Although all spectra largely overlap, the spectrum profile depends on the base sequence. The spectrum of (dA)₂₀·(dT)₂₀ is very similar to that of poly(dA)·poly(dT) and the spectrum of (dAdT)₁₀·(dAdT)₁₀ closely resembles that of poly(dAdT)·poly(dAdT). A closer look in the absorption spec-

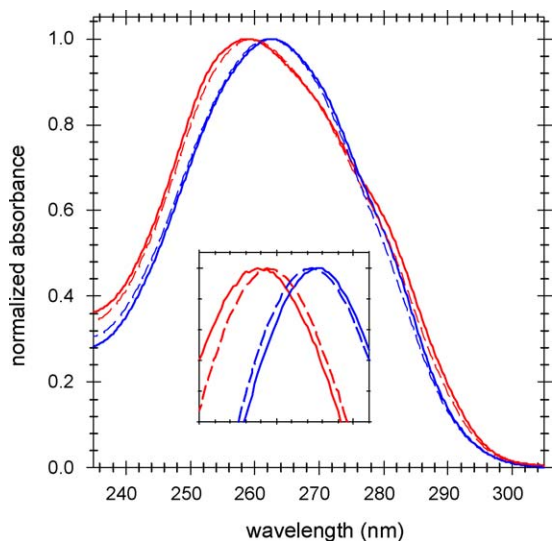


Fig. 2. Normalized absorption spectra of poly(dA)·poly(dT) (solid red line), (dA)₂₀·(dT)₂₀ (dashed red line), poly(dAdT)·poly(dAdT) (solid blue line), (dAdT)₁₀·(dAdT)₁₀ (dashed blue line).

tra (inset in Fig. 2) reveals that the effect of the base sequence is more pronounced for the polymers compared to the oligomers. The position of absorption maxima are given in Table 1. Such a relative position is predicted by a theoretical study performed in the frame of the exciton theory combining data from quantum chemistry calculations and molecular dynamics simulations [25,27]. It was explained by the delocalization of the Franck–Condon excited states over several bases induced by dipolar coupling (Frenkel excitons). As the dipolar coupling depends on the orientation of the transition dipoles, it is sensitive to the geometrical arrangement of the chromophores and, consequently, to the base sequence. Although the formation of excitons induced by dipolar coupling explains the sequence dependence of the absorption maxima, it does not account for the observed hypochromism, which is also sequence dependent [32]. In contrast, charge resonance and charge transfer interactions acting between bases provide a satisfactory interpretation for this effect [33,34].

According to the above reasoning we deduce that the footprint of electronic coupling is more visible in the spectra of the polymers compared to those of the oligomers. This is also reflected in the excited state relaxation of the examined double strands studied by fluorescence upconversion. For example, it was reported that the fluorescence decay recorded at 330 nm for (dA)₂₀·(dT)₂₀ is slower than that obtained for an equimolar mixture of dAMP and TMP [16]. Fig. 3 shows that this trend is accentuated in the fluorescence decay of poly(dA)·poly(dT).

3.2. Fluorescent impurities

We found that some oligomers contained fluorescent impurities. These were not easy to recognize at the first glance. As a matter of fact, a difference in the fluorescence spectra or in the fluorescence decays between nucleotides and single or dou-

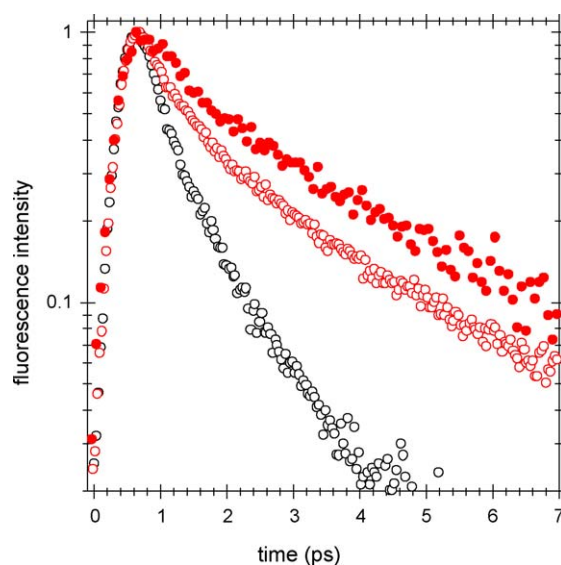


Fig. 3. Normalized fluorescence decays recorded at 330 nm by the upconversion technique: (dA)₂₀·(dT)₂₀ (red open circles), poly(dA)·poly(dT) (red full circles) and an equimolar mixture of the nucleotides dAMP and TMP (black open circles); $\lambda_{\text{ex}} = 267$ nm.

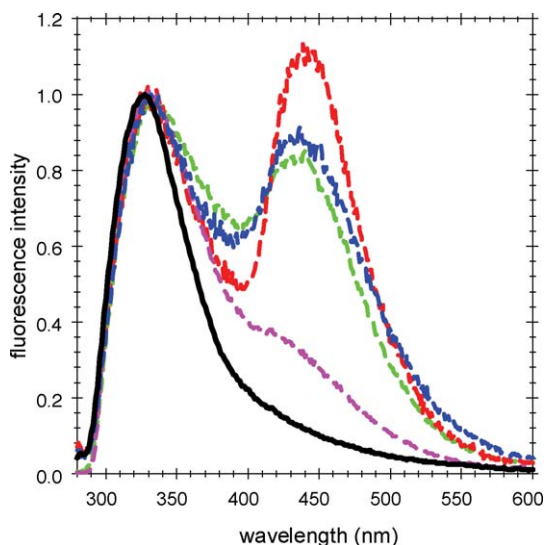


Fig. 4. Steady-state fluorescence spectra recorded for different batches of $(dA)_{20} \cdot (dT)_{20}$ (colour lines). The fluorescence spectrum of poly(dA)·poly(dT), which was found to be identical for all batches, is shown in black; $\lambda_{ex} = 255$ nm.

ble stranded oligomers could be interpreted as a cooperative effect. We have been able to distinguish between a cooperative property and a fluorescent impurity by performing a series of tests. They are illustrated below using $(dA)_{20} \cdot (dT)_{20}$ as an example.

The fluorescence spectra of $(dA)_{20} \cdot (dT)_{20}$ recorded for different batches are presented in Fig. 4. They are characterized by two emission bands. One of them peaks around 330 nm, wavelength which coincides with the maximum of TMP fluorescence spectrum [8]. The second peak is located around 450 nm and could be attributed to “excimer” emission. However, the 450 nm peak is still present above the melting temperature. The relative intensities of the two peaks changes with the excitation wavelength and, most importantly, they vary from one batch to the other. In contrast, the fluorescence spectra recorded for at least six different batches of poly(dA)·poly(dT) were independent of the excitation wavelength and contain just one emission band peaking at 327 nm (Fig. 4). On the basis of these observations we concluded that $(dA)_{20} \cdot (dT)_{20}$ contains a fluorescent impurity. This impurity is certainly present in very low concentration because the batches characterized by different fluorescence spectra (Fig. 4) gave identical absorption spectra.

Due to the fluorescent impurity the decays of $(dA)_{20} \cdot (dT)_{20}$ recorded by the time-correlated single photon counting technique at 420 nm are longer than those of poly(dA)·poly(dT) (Fig. 5). Despite this fact, the decays of the oligomer recorded by means of the upconversion technique are shorter than those of the polymer at all wavelengths because the latter technique is not sensitive to long lived emitting species with low amplitude. We recall that the fluorescence decays of poly(dA)·poly(dT) are quite complex. They are composed of large amplitude short lived components which are determined by the upconversion technique and weak amplitude long lived components determined by TCSPC [17].

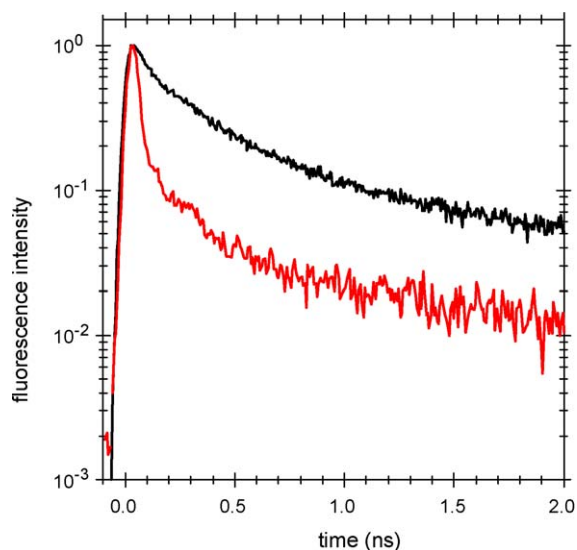


Fig. 5. Normalized total fluorescence decays recorded at 420 nm for $(dA)_{20} \cdot (dT)_{20}$ (black) and poly(dA)·poly(dT) (red) by time-correlated single photon counting $\lambda_{ex} = 267$ nm.

4. Excitation of helices containing photoproducts

In this section we propose an evaluation of the probability that successive laser pulses, necessary for recording a time-resolved signal, excite helices already containing a photoproduct. This probability depends on various parameters, such as laser intensity and repetition rate, sensitivity of the measurement, concentration and volume of the studied solution. We illustrate this by two examples of how excitation of damaged helices alters the fluorescence decays.

One photon absorption by model helices leads to the formation of photoproducts with various quantum yields ϕ . For the most commonly studied model helices, the highest ϕ is reported for the formation of cyclobutane dimers in the single strand $(dT)_{20}$ (3×10^{-2}) [5] and the lowest for the formation of A–T adducts in the double stranded helix poly(dAdT)·poly(dAdT) (ca. 10^{-4}) [35]. Moreover, in laser experiments, one or two photon ionization of the DNA helices may also occur [5,36–40], resulting in the formation of oxidation products. The majority of these reaction products absorb, more or less, at the same spectral area as the initial systems and their formation cannot easily be detected just by monitoring the absorption spectra before and after the time-resolved experiment. Therefore, it is important to use other criteria for checking the alteration of the compounds during the measurement.

We have estimated the accumulation of photoproducts during a time-resolved experiment by calculating the molar fraction $R(n)$ of helices undergoing a photoreaction as a function of the number of laser shots n . $R(n)$ is given by the ratio $[\text{photoproduct}]_n / [\text{helices}]$ where the nominator and the denominator correspond to the photoproduct concentration present in the solution after n laser shots and the total concentration of helices, respectively. We are interested in the number of shots resulting to the creation of a photoproduct in less than 10% of the helices. Under these conditions, the number of absorbed photons

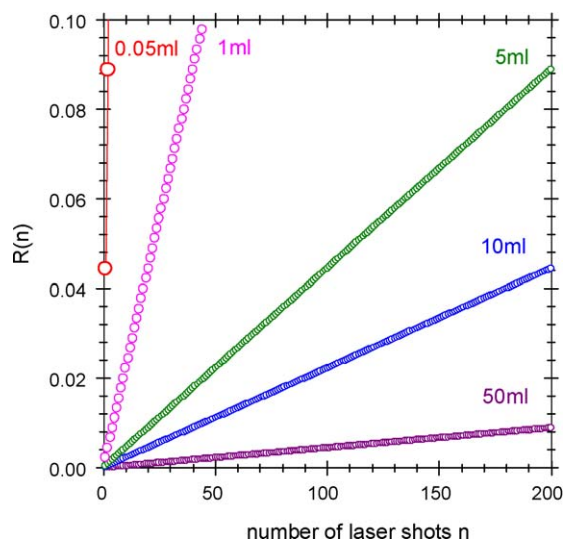


Fig. 6. Molar fraction of helices containing one photoproduct $R(n)$ as a function of the laser shots n in a nanosecond flash photolysis experiment for various total volumes of solution circulating through a flow cell. Helix concentration: 10^{-5} M; absorbed energy per laser pulse at 267 nm: 2 mJ; $\phi = 5 \times 10^{-3}$; $V_{\text{irr}} = 0.05$ ml.

per shot remains approximately constant. Thus, we write:

$$[\text{photoproduct}]_n = \frac{n\phi[P_a]V_{\text{irr}}}{V_{\text{tot}}}$$

where ϕ is the quantum yield for photoproduct formation, $[P_a]$ the number of absorbed photons (in einstein/l), V_{irr} the volume of the solution directly irradiated by the laser pulses and V_{tot} is the total volume of the solution circulating through a flow cell or being continuously stirred during the experiment.

Fig. 6 shows plots corresponding to nanosecond flash photolysis experiments for different volumes V_{tot} . The $R(n)$ values are presented for n up to 200, which is a typical number for signal averaging in order to obtain transient absorption decays with an acceptable signal to noise ratio. The parameters used in the simulations (helix concentration: 10^{-5} M; absorbed energy per laser pulse at 267 nm: 2 mJ; $\phi = 5 \times 10^{-3}$) are inspired from our recent work on oligomers composed of 20 bases (single strands) or 20 base pairs (double strands) [5,23]. We observe that when the same small volume of solution is excited by successive pulses ($V_{\text{irr}} = V_{\text{tot}} = 0.05$ ml), two laser shots are sufficient to damage 9% of the helices. If 50 ml of solution are circulating via a flow cell, less than 1% of the helices contain a photoproduct after 200 shots and the obtained signals are considered to be reliable.

In the simulations described above several parameters can be varied allowing the determination of the optimal conditions depending on the type of time-resolved experiments. In all cases, we judge a measurement to be acceptable if successive signals recorded for the same total volume of solution are identical. An example is given in Fig. 7 where the fluorescence decays recorded by TCSPC for poly(dA)·poly(dT) at 420 nm with parallel polarization are shown. In this experiment, we have adopted a protocol where we defocused the laser beam in order to decrease the pulse intensity to less than 10 kW/cm^2 (lower than the sensitivity of our powermeter). Moreover, 3 ml of solution were

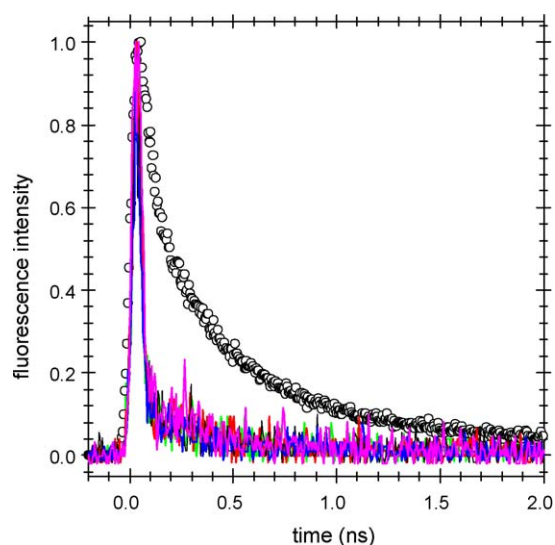


Fig. 7. Normalized fluorescence decays (parallel polarization) recorded at 420 nm for poly(dA)·poly(dT) by time-correlated single photon counting; $\lambda_{\text{ex}} = 267$ nm. Black circles: usual operating conditions (no stirring; pulse intensity: 200 kW/cm^2). Colour lines correspond to 10 successive measurements (300 s each) performed under continuous stirring of the solution ($V_{\text{tot}} = 3$ ml) and with a laser power intensity lower than 10 kW/cm^2 .

continuously stirred during the measurement. Under these conditions, 10 successive decays (colour lines in Fig. 7) perfectly overlap. If the experiment is performed under experimental conditions currently used in TCSPC (no defocusing, no stirring), successive decays become longer and longer. This is mainly due to the formation of (6–4) thymine dimers whose fluorescence maximum is located around 400 nm [41]. Their fluorescence quantum yield is 10^{-2} , i.e. two orders of magnitude higher than that of the studied double helix. For comparison, an average decay recorded under such conditions is also shown in Fig. 7. As can be seen, it is much longer than the decays recorded according to our protocol. It is important to stress that the presence of the (6–4) photo-adducts is relatively easy to detect because their photophysical and photochemical properties are rather well characterized contrary to other photoproducts.

As mentioned in Section 1, the formation of photoproducts may not only contribute to the fluorescence decays by their own emission but also change the excited state relaxation of the DNA. An example is illustrated in Fig. 8 and concerns the fluorescence decays of (dA)₂₀·(dT)₂₀ at 330 nm recorded by the upconversion technique. The decay obtained using a rotating cell containing 0.4 ml of solution is clearly shorter than the decay obtained using a flow cell allowing the circulation of 20 ml of solution. The fluorescence of (6–4) thymine dimers which decays on the nanosecond time-scale (Fig. 7) is not responsible for the observed shortening of the decay. In contrast, this shortening can be explained by partial denaturation of the double strand provoked by the accumulation of both (6–4) photo-adducts and cyclobutane dimers which are not fluorescent. As a matter of fact, we have reported that the fluorescence decays of (dA)₂₀ and (dT)₂₀, detected by the upconversion technique at 330 nm, are shorter than that of (dA)₂₀·(dT)₂₀ [16].

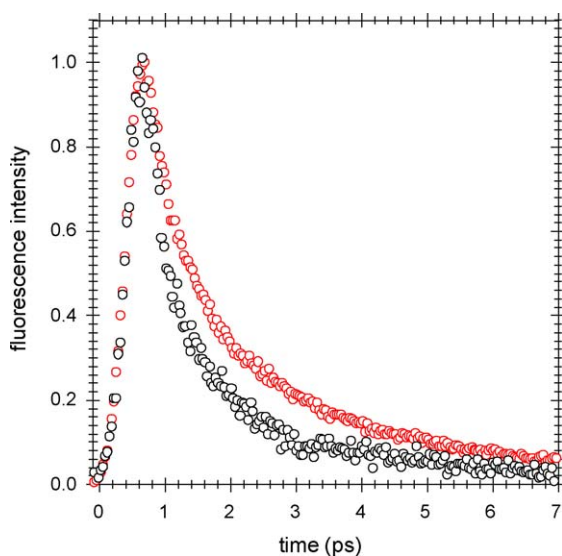


Fig. 8. Normalized total fluorescence decays recorded at 330 nm by the up-conversion technique for $(dA)_{20}-(dT)_{20}$. Black circles: rotating cell containing 0.04 ml. Red circles: 20 ml of solution continuously circulating through a flow cell.

5. Conclusions and comments

We have outlined some pitfalls which may hamper time-resolved studies of DNA helices and described some tricks we have developed in order to avoid them. We illustrate our experience by examples from experiments performed on double helices containing only adenine–thymine base pairs.

First, we stress the importance of controlling the quality of samples by means of techniques available in a photochemistry laboratory. Thus, careful inspection of the steady-state absorption and fluorescence spectra and their temperature dependence constitute an important prerequisite for any laser experiment. The degree of hypochromicity and the precise position of the absorption maximum are crucial criteria which should be mentioned explicitly in every scientific paper. On the basis of these criteria, it appears that polymers are better models for the DNA double helix than the oligomers which contain relatively more unpaired bases.

The second problem we have pointed out is the damage of the helices occurring during the laser experiments. We have proposed a simplified evaluation of this damage allowing the adjustment of experimental parameters (laser repetition rate, irradiated surface, helix concentration, duration of the experiment, ...) and, accordingly, the determination of the volume of the solution necessary to obtain reliable signals. Such an evaluation may be a valuable guide for the design of the experiment. However, the ultimate test is to check if repetitive signals recorded with the same solution are reproducible.

Given the complexity of the involved processes, coordinated efforts of various groups and techniques are necessary. We are convinced that the first step in this direction is to establish a set of commonly accepted experimental protocols. By the present contribution we wish to share our own experience which we

hope will be enriched by discussions with other groups working in the same field.

References

- [1] N. Dumaz, C. Drougard, A. Sarasin, Proc. Natl. Acad. Sci. U.S.A. 90 (1993) 10529–10533.
- [2] E. Sage, Photochem. Photobiol. 57 (1993) 163–174.
- [3] J. Cadet, M. Berger, T. Douki, B. Morin, R.S.J.L. Ravanat, S. Spinelli, Biol. Chem. 378 (1997) 1275–1286.
- [4] J. Cadet, P. Vigny, in: H. Morrison (Ed.), Bioorganic Photochemistry, John Wiley & Sons, New York, 1990, pp. 1–272.
- [5] S. Marguet, D. Markovitsi, J. Am. Chem. Soc. 127 (2005) 5780–5781.
- [6] G. Porter, Nobel Lect. (1967) 1–23.
- [7] D. Voet, W.B. Gratzer, R.A. Cox, P. Doty, Biopolymers 1 (1963) 193–208.
- [8] D. Onidas, D. Markovitsi, S. Marguet, A. Sharonov, T. Gustavsson, J. Phys. Chem. B 106 (2002) 11367–11374.
- [9] J.-M.L. Pecourt, J. Peon, B. Kohler, J. Am. Chem. Soc. 123 (2001) 10370–10378.
- [10] J.-M.L. Pecourt, J. Peon, B. Kohler, J. Am. Chem. Soc. 122 (2000) 9348–9349.
- [11] J. Peon, A.H. Zewail, Chem. Phys. Lett. 348 (2001) 255–262.
- [12] T. Gustavsson, A. Sharonov, D. Markovitsi, Chem. Phys. Lett. 351 (2002) 195–200.
- [13] T. Gustavsson, A. Sharonov, D. Onidas, D. Markovitsi, Chem. Phys. Lett. 356 (2002) 49–54.
- [14] A. Sharonov, T. Gustavsson, S. Marguet, D. Markovitsi, Photochem. Photobiol. Sci. 2 (2003) 362–364.
- [15] A. Sharonov, T. Gustavsson, V. Carré, E. Renault, D. Markovitsi, Chem. Phys. Lett. 380 (2003) 173–180.
- [16] D. Markovitsi, A. Sharonov, D. Onidas, T. Gustavsson, Chem. Phys. Chem. 3 (2003) 303–305.
- [17] D. Markovitsi, D. Onidas, T. Gustavsson, F. Talbot, E. Lazzarotto, J. Am. Chem. Soc. 127 (2005) 17130–17131.
- [18] C.E. Crespo-Hernández, B. Cohen, B. Kohler, Nature 436 (2005) 1141–1144.
- [19] D. Markovitsi, F. Talbot, T. Gustavsson, D. Onidas, E. Lazzarotto, S. Marguet, Nature 441 (2006), doi:10.1038/nature04903.
- [20] R. Plessow, A. Brockhinke, W. Eimer, K. Kohse-Hoinghaus, J. Phys. Chem. B 104 (2000) 3695–3704.
- [21] S. Georghiou, T.D. Bradrick, A. Philippetis, J. Biochem. Biophys. 70 (1996) 1909–1922.
- [22] D. Markovitsi, T. Gustavsson, A. Sharonov, Photochem. Photobiol. 79 (2004) 526–530.
- [23] S. Marguet, D. Markovitsi, F. Talbot, J. Phys. Chem. B (2006), doi:10.1021/jp062578m.
- [24] B. Bouvier, T. Gustavsson, D. Markovitsi, P. Millié, Chem. Phys. 275 (2002) 75–92.
- [25] B. Bouvier, J.P. Dognon, R. Lavery, D. Markovitsi, P. Millié, D. Onidas, K. Zakrzewska, J. Phys. Chem. B 107 (2003) 13512–13522.
- [26] D.F. Lewis, X. Liu, Y. Wu, X. Zuo, J. Am. Chem. Soc. 125 (2003) 12729–12731.
- [27] E. Emanuele, D. Markovitsi, P. Millié, K. Zakrzewska, Chem. Phys. Chem. 6 (2005) 1387–1392.
- [28] E. Emanuele, K. Zakrzewska, D. Markovitsi, R. Lavery, P. Millié, J. Phys. Chem. B 109 (2005) 16109–16118.
- [29] T. Douki, D. Angelov, J. Cadet, J. Am. Chem. Soc. 123 (2001) 11360–11366.
- [30] M. Riley, B. Maling, M.J. Chamberling, J. Mol. Biol. 20 (1966) 359–389.
- [31] P.O.P. Ts'o, A. Seymour, S.A. Rapaport, F.J. Bollum, Biochemistry 5 (1966) 4153–4170.
- [32] E.S. Pysh, J.L. Richards, J. Chem. Phys. 57 (1972) 3680–3685.
- [33] E.B. Starikov, Modern Phys. Lett. B 18 (2004) 825–831.
- [34] D. Varsano, R. Di Felice, M.A.L. Marques, A. Rubio, J. Phys. Chem. B 110 (2006) 7129–7138.

- [35] S.N. Bose, R.J.H. Davies, S.K. Sethi, J.A. McCloskey, *Science* 220 (1983) 723–725.
- [36] D.N. Nikogosyan, *Int. J. Radiat. Biol.* 57 (1990) 233–299.
- [37] M. Wala, E. Bothe, H. Görner, D. Schulte-Frohlinde, *J. Photochem. Photobiol. A: Chem.* 53 (1990) 87–108.
- [38] L.P. Candeias, P. O'Neill, G.D.D. Jones, S. Steenken, *Int. J. Radiat. Biol.* 61 (1992) 15–20.
- [39] Q. Zhu, P.R. LeBreton, *J. Am. Chem. Soc.* 122 (2000) 12824–12834.
- [40] H. Fernando, G.A. Papandonakis, N.S. Kim, P.R. LeBreton, *Proc. Natl. Acad. Sci. U.S.A.* 95 (1998) 5550–5555.
- [41] J. Blais, T. Douki, P. Vigny, J. Cadet, *Photochem. Photobiol.* 59 (1994) 402–404.